Probing Defect Sites on the CeO_2 Surface with Dioxygen

Vladimir V. Pushkarev, Vladimir I. Kovalchuk, and Julie L. d'Itri*

Department of Chemical Engineering, University of Pittsburgh, Pittsburgh, Pennsylvania 15261

Received: September 30, 2003; In Final Form: February 2, 2004

In situ Raman spectroscopy of adsorbed dioxygen was used to characterize electron defects on the surface of nanocrystalline cerium oxide that was partially reduced with H_2 and CO. Via $^{16}O/^{18}O$ isotope substitution, the bands in the range of 1135−1127 and 877−831 cm^{-1} were assigned to the O−O stretching vibration of dioxygen species bound to one- and two-electron defects on the CeO_2 surface to form superoxide (O_2^-) and peroxide (O_2^{2-}) species, respectively. A band at 357 cm^{-1} was attributed to the cerium−oxygen vibration of the adsorbed superoxides, O_2^-, whereas the bands at 538 and 340 cm^{-1} were assigned to the asymmetric and symmetric cerium−oxygen vibrations of the surface peroxides, O_2^{2-}, respectively. The dynamics of the defect annihilation that results from surface reoxidation by adsorbed dioxygen species during temperature-programmed experiments allowed peroxide species adsorbed on isolated and aggregated two-electron defects to be distinguished. A general approach to investigate the reactivity of different surface dioxygen species toward reductants was demonstrated using CO oxidation as a probe reaction.

Introduction

An understanding of the structure and dynamics of the surface of solids during exposure to different gaseous media is of paramount importance in predicting catalytic performance. In the case of oxides, surface coordinatively unsaturated metal cations and oxygen anion vacancies are likely participants in the activation of reactants in catalytic reactions.[1−6] Infrared spectroscopy of probe molecules, often CO and NO, is a well-established approach to characterize donor−acceptor properties of surface defects in solids.[5] However, the molecules adsorbed on the oxide surfaces are prone to decomposition and oxidation, which usually modifies the properties of the surface under investigation.[5] In addition, both CO and NO have a limited ability to probe the electron structure of the adsorption sites, and hence, distinguishing between different surface electron defects is not possible.[7−10]

There are advantages to using dioxygen to characterize oxide surface defects. The adsorption of O_2 on one- and two-electron defects results in the formation of surface superoxide, O_2^-, and peroxide, O_2^{2-}, species with vibrational features essentially different from each other and from gaseous and physisorbed dioxygen.[5,11,12] Moreover, both peroxide and superoxide species are postulated to be kinetically significant intermediates in a number of oxidation reactions, and a detailed study of these species is, therefore, important to understand the mechanism of oxidation reactions catalyzed by oxides.[2,6,13,14]

Our goal was to probe the properties of oxide surfaces with dioxygen. In situ Raman spectroscopy was used to investigate dioxygen species adsorbed on a CeO_2 surface that was partially reduced with CO and H_2, the dynamics of the surface reoxidation during temperature-programmed experiments, and the reactivity of the surface dioxygen species toward CO. Cerium oxide was chosen because it is an industrially significant catalyst, catalyst support, and promoter for different catalytic reactions, including complete and partial oxidation of CO and hydrocarbons and automotive exhaust catalysis.[4,15−19] Among the vibrational techniques, Raman spectroscopy is well suited to study the molecular forms of adsorbed oxygen. The high polarizability and the low dipole momentum of the O−O bond in the homoatomic O_2 molecule contribute to the relatively high extinction for the stretching O−O bond vibration in Raman spectroscopy.[20] In addition, the metal−oxygen vibrations of adsorbed dioxygen species in the range of 300−600 cm^{-1} can be monitored by Raman spectroscopy; these vibrations are usually obscured in the IR spectra because the majority of metal oxides completely absorb the IR irradiation below 700−800 cm^{-1}.[5]

Experimental Section

Cerium dioxide, CeO_2 (>99.9%), was provided by Rhodia. Prior to use, the CeO_2 was calcined in air at 823 K for 12 h in a standard muffle furnace. The BET surface area after calcination, measured by N_2 physisorption at 77 K with ASAP 2010 volumetric sorption analyzer (Micromeritics), was 127 $m^2\ g^{-1}$. The average crystallite size determined from the (111) and (220) XRD lines broadening using the Scherrer equation was 9.7 nm.

The reagent-grade He (Air Products, >99.998%) was purified of water and oxygen traces by passing it through a deoxidant OxyTrap filter and through a 0.5-nm molecular sieve column (both Alltech). The trace contaminants of water and carbon dioxide in 10% O_2 in He (UHP, Liquid Carbonix), 5% H_2 in He (UHP, Penn Oxygen) gas mixtures, and in CO (Air Products, >99.995%) were removed by 0.5-nm molecular sieve columns (Varian). The $^{18}O_2$ (Isotec, >99.9% of $^{18}O_2$) gas was used as received.

The Raman spectra were acquired with a Renishaw System 2000 confocal Raman spectrometer equipped with a Leica DMLM microscope and a 514.5-nm Ar^+ ion laser as an excitation source. The laser power at the sample was 1.5 mW. A ×50 objective of 8-mm optical length was used to focus the depolarized laser beam onto a 3−5-μm spot on the sample surface and to collect the backscattered light. The light was dispersed by a single-stage spectrometer with an 1800-groove mm^{-1} grating and acquired by an air-cooled 578 × 238 pixels

* Author to whom correspondence should be addressed. Phone: 412-624-9634. Fax: 412-624-9639. E-mail: jditri@pitt.edu.

10.1021/jp0311254 CCC: $27.50
Published on Web 04/06/2004

CCD array detector. The Raman scattering was collected in a static-scan mode in the 800−1700 cm^{-1} spectral region with a resolution better than 4 cm^{-1}. Ten scans were accumulated for each spectrum during a total scanning time of 100 s. Spectra were also collected in the extended-scan mode over the spectral range of 100−4000 cm^{-1}, for which the grating was stepped synchronously with the shifting of charge in the CCD array. Ten scans were accumulated in this mode during a total scanning time of approximately 10 min. The spectra were processed, including deconvolution when necessary, with GRAMS/32 software from Galactic Industries, Inc.

The Raman experiments were conducted in a temperature-controlled THMS 600 in situ cell from Lincam Scientific that operated in the 77−873-K temperature range and allowed optical access through a thin (0.2 mm) fused quartz window. To avoid sample overheating with the laser beam, the cell was moved backward and forward during spectra acquisition at a velocity of 1 mm s^{-1}. Additional experiments were performed in which the intensities of the Stokes and anti-Stokes spectral components in the range of 77−300 K were analyzed.[21] These experiments showed that the actual temperature of the stationary reduced sample exceeded the thermocouple reading by less than 10 K (see Supporting Information).

Approximately 25 mg of CeO_2 in the form of a microcrystalline powder was pressed under 90 MPa pressure into a 10 mm diameter pellet; the pellet was mounted into the cell. The reaction gases were mixed prior to admission to the Raman cell, and the desired flow rate of each gas was maintained within ±1 cm^3 min^{-1} with mass flow controllers (Brooks model 5850E). The total gas flow rate was maintained at 100 cm^3 min^{-1} in all experiments. Before each experiment, the sample was heated in a flow of a gas mixture containing 10% of O_2 in He from ambient temperature to 673 K at a rate of 10 K min^{-1} and held at 673 K for 1 h. Then, the sample was cooled to ambient temperature under the same gas flow. The CeO_2 sample pretreated as described above is designated as oxidized in the remainder of the paper.

For the O_2 adsorption on oxidized CeO_2 experiments, the sample was cooled at a rate of 100 K min^{-1} from ambient temperature to 93 K under a flow of pure He. Then, 10% of the He flow was substituted by O_2, and the sample was heated from 93 to 673 K at a rate of 5 K min^{-1}, pausing at specified temperatures to collect spectra. Prior to acquiring a spectrum, the sample was allowed to equilibrate with the gas phase for 15 min at each temperature.

The O_2 adsorption experiments with CeO_2 samples that had been prereduced with H_2 or CO at a specific temperature were performed as follows. An oxidized CeO_2 sample was heated under a flow of either 5% H_2 or 5% CO in He at a rate of 10 K min^{-1} from ambient temperature to one of the following temperatures: 473, 573, or 673 K, and held at that temperature for 1 h. Then, the gas flow was substituted for a flow of pure He for 2 min before the sample was cooled in He to 93 K at a rate of 100 K min^{-1}. At 93 K, 10% of the He flow was substituted by O_2 and the sample was held at 93 K for 15 min prior to acquiring a spectrum. A similar experimental procedure was used for the $^{18}O_2$ adsorption experiments; at 93 K, a flow of 10% $^{18}O_2$ in He was admitted to the in situ cell containing the CeO_2 sample that was prereduced in a flow of either 5% H_2 or 5% CO in He at 673 K for 1 h.

Prior to the temperature-programmed experiments, a H_2- or CO-reduced CeO_2 sample was cooled to 93 K at a rate of 100 K min^{-1} in a flow of He. At 93 K, 10% of the He flow was substituted by O_2 and the sample was held at that temperature for 15 min. Then, the sample was heated from 93 to 673 K at a rate of 5 K min^{-1} while flowing either 10% O_2 in He or pure He, and the spectra were collected at 20 K increments. Each of the indicated temperatures corresponds to the temperature at the end of spectrum acquisition.

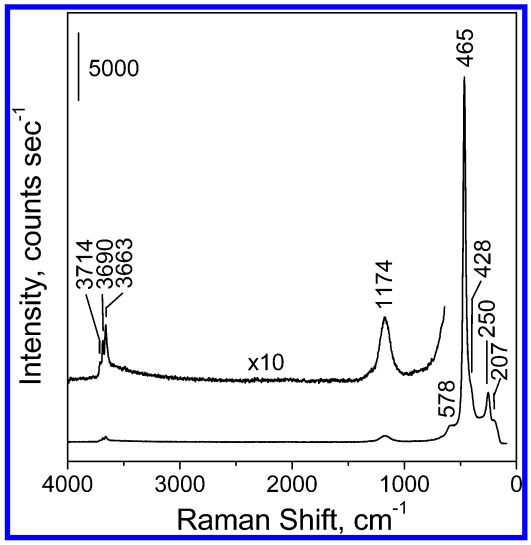

Figure 1. Raman spectrum of oxidized CeO_2.

Results

The Raman spectrum of the oxidized CeO_2 consisted of a strong band at 465 cm^{-1} (Figure 1). This band has been attributed to the vibrational mode of the F_{2g} symmetry, the only Raman-active mode of the perfect cubic fluorite lattice (space group O_h).[22,23] In addition, there is a group of very weak bands at 207, 250, 428, 578, and 1174 cm^{-1}. These second-order bands arise from a mixing of A_{1g}, E_g, and F_{2g} vibrational modes of the CeO_2 lattice. The first- and second-order CeO_2 bands will not be discussed hereinafter. The integral intensity of the band at 1174 cm^{-1} could be used as an internal standard for quantitative interpretation of Raman spectra under the assumption that exposure of CeO_2 to H_2 or CO reduces the surface or subsurface oxide layers and does not affect substantially the bulk CeO_2 structure.[24−28] There were also bands at 3663, 3690, and 3714 cm^{-1}, which were previously assigned to the O−H stretching vibrations of two types of bicoordinated and one type of monocoordinated surface hydroxyl groups, respectively.[12,29] No other bands were detected in the 100−4000-cm^{-1} spectral range.

When the oxidized CeO_2 pellet was exposed to an O_2-containing flow at temperatures between 93 and 673 K, no bands attributable to chemisorbed dioxygen species were detected (Figure 2). In addition to the band of CeO_2 at 1174 cm^{-1}, a band at 1551 cm^{-1} was the only other band that was observed at temperatures below 153 K in the range of 100−1700 cm^{-1}. The 1551-cm^{-1} band was assigned previously to physisorbed molecular oxygen.[11]

The Raman spectra associated with the interaction of O_2 with the CeO_2 surface that was pre-exposed to H_2 at 473, 573, and 673 K is shown in Figure 3A. The treatment in a flow of 5% H_2 in He at 473 K for 1 h (Figure 3A, spectrum 1) did not alter the positions of the vibrational bands compared to the oxidized CeO_2 (Figure 2). The bands at 1551 and 1174 cm^{-1} were the only ones observed for both samples in the region of 800−1600 cm^{-1}. However, an asymmetry of the 1174 cm^{-1} band on its lower wavenumber side suggests the presence of another species. After reduction at 573 K, two bands at 1127 and 1135

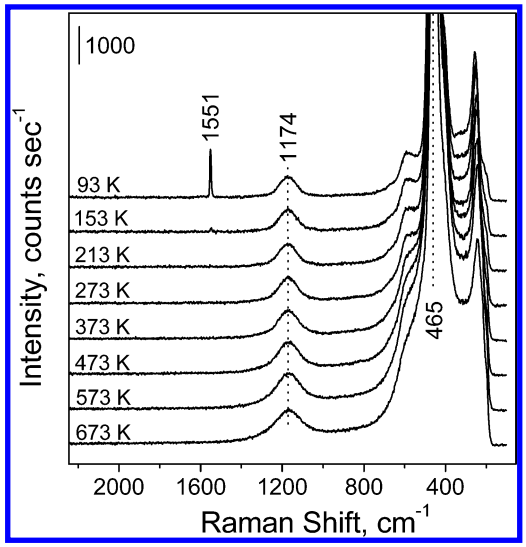

Figure 2. Dioxygen adsorption on oxidized CeO_2. The CeO_2 pellet was heated under 10% O_2 in He flow from 93 to 673 K at a rate of 5 K min^{-1}, and the spectra were collected at each of the specified temperatures.

cm^{-1} were clearly visible along with the bands at 1551 and 1174 cm^{-1} and a new low-intensity band at 831 cm^{-1} (Figure 3A, spectrum 2). When the reduction temperature was increased to 673 K, O_2 adsorption resulted in an increase in intensity of the bands at 1135, 1127, and 831 cm^{-1}. In addition, new low-intensity bands at 1487, 538, and 357 cm^{-1} and shoulders at 860 and 340 cm^{-1} appeared in the spectrum (Figure 3A, spectrum 3; Figure 4, spectrum 1).[30] Concomitantly, the band at 1174 cm^{-1} decreased in intensity with a simultaneous darkening of the sample as the reduction temperature was increased. The intensity ratio between the 1551- and 1174-cm^{-1} bands decreased by a factor of 2 when the reduction temperature was increased from 473 to 673 K.

In general, the bands resulting from O_2 adsorption on the CeO_2 pellet reduced with CO were more intense at lower reduction temperatures and less intense at higher reduction temperatures than those observed for CeO_2 reduced with H_2 (Figure 3B). Exposure of the CeO_2 pellet reduced in CO at 473 K to an O_2-containing flow resulted in a Raman spectrum with bands at 1127, 1135, 831, and 860 cm^{-1} and a band for physisorbed O_2 at 1551 cm^{-1} (Figure 3B, spectrum 1). An additional band at approximately 877 cm^{-1} was detected for the CeO_2 samples that were reduced at 573 and 673 K (Figure 3B, spectra 2−3). When the reduction temperature was increased, there was a decrease in the intensity of the band of CeO_2 at 1174 cm^{-1} and a decrease in the ratio of the 1551- and 1174-cm^{-1} band intensities. Apparently, using a high reduction temperature modifies acid−base properties of the surface. According to quantum chemical considerations,[31] both acidic and basic centers are responsible for the dioxygen adsorption. Similar to the CeO_2 samples reduced with H_2, the Raman spectra of the CO-reduced CeO_2 contained weak and broad bands at approximately 340 and 538 cm^{-1} (not shown).[30]

All the bands associated with adsorbed dioxygen exhibited a redshift when $^{18}O_2$ was used as the adsorbate instead of $^{16}O_2$ (Figure 4). The isotopic shift for physisorbed oxygen (a band at 1551 cm^{-1} for $^{16}O_2$ adsorption) was 86 cm^{-1}. The bands observed at 1487, 1135, 1127, and 831 cm^{-1} and the shoulder at 860 cm^{-1} after $^{16}O_2$ adsorption shifted by 75, 64, 62, 45, and 51 cm^{-1}, respectively, after adsorption of $^{18}O_2$. The low-frequency bands at 357 and 340 cm^{-1} shifted to 342 and 324 cm^{-1}, respectively. The band at 538 cm^{-1} shifted to approximately 529 cm^{-1} upon adsorption of $^{18}O_2$; it was difficult to determine accurately the magnitude of the shift because this band was broad and very weak.

The thermal stability of the different bands resulting from dioxygen adsorption was investigated by the temperature-programmed experiments for CeO_2 samples reduced with both H_2 (Figure 5) and CO (Figure 6) at 673 K. A continuous purge of the H_2-reduced sample with a He flow at 93 K led to the complete disappearance of the band at 1551 cm^{-1} (Figure 5A), while the intensity of bands at 1487, 1135, 1127, 860, 831, 538, 357, and 340 cm^{-1} did not change. Once heating was started, the bands at 1487, 1135, and 1127 cm^{-1} gradually decreased in intensity until they were no longer detectable at temperatures above 300 K. The thermal dependence of the band intensities in the range of 831−877 cm^{-1} was more complex. The band at 831 cm^{-1} gradually increased in intensity in the temperature range of 93−350 K. The intensity reached a maximum at approximately 350 K and then decreased to the background level by 530 K. The band at 860 cm^{-1} increased as the temperature increased from 93 to 220 K. When the temperature exceeded 220 K, the intensity of the band at 860 cm^{-1} decreased and was undetectable at 400 K. In the range of 877−831 cm^{-1}, there was also a band at 877 cm^{-1}; its intensity gradually decreased with temperature to reach the background level at approximately 350 K. The thermal stability of the bands at 1487 and 357 cm^{-1} was similar to the stability of the bands at 1135−1127 cm^{-1}, and the stability of the bands at 538 and 340 cm^{-1} correlated with the stability of the bands at 831−877 cm^{-1} (Figure 5B). The intensity of the band at 1174 cm^{-1} increased during the temperature-programmed experiment until approximately 540 K and remained constant thereafter. Using a flow of 10% O_2 in He instead of pure He did not affect the dynamics of the band intensities but slightly increased the temperature at which the maximum intensity of the band at 1174 cm^{-1} was obtained (Figure 5C).

Similar to the H_2-reduced CeO_2, a continuous purge of the CO-reduced sample with a He flow at 93 K resulted in the complete disappearance of the band at 1551 cm^{-1}, while the other bands associated with O_2 adsorption remained unchanged (Figure 6A). Once the heating was started, the bands at 1487, 1135, and 1127 cm^{-1} decreased in intensity and were undetectable at temperatures as low as 130 K. The intensities of the three bands at 877, 860, and 831 cm^{-1} increased gradually as the temperature increased from 93 to 300 K. A further increase in temperature resulted in the decrease in intensity of the bands at 877 and 860 cm^{-1} and an increase in the intensity of the band at 831 cm^{-1}. At temperatures above 400 K, the bands at 877 and 860 cm^{-1} were undetectable. The intensity of the 831-cm^{-1} band reached its maximum at 360 K and then decreased in intensity until it was undetectable at temperatures above 520 K. The intensity of the band at 1174 cm^{-1} increased with temperature to a maximum value at 520 K and remained constant thereafter.

When a flow of 10% O_2 in He was used instead of pure He flow (Figure 6B), the bands at 1477, 1135, and 1131 cm^{-1} increased with temperature to a maximum at approximately 173 K and then decreased. At temperatures greater than 273 K, these bands were undetectable. The intensity of the bands at 877, 860, and 831 cm^{-1} increased from 93 to 190 K. At temperatures above 190 K, the band at 877 cm^{-1} decreased steadily to a minimum at 290 K and passed through the second maximum at 320 K to be undetectable at 420 K. The bands at 860 and 831 cm^{-1} passed through a maximum at 290 and 370 K, respectively, and they were undetectable at approximately 500

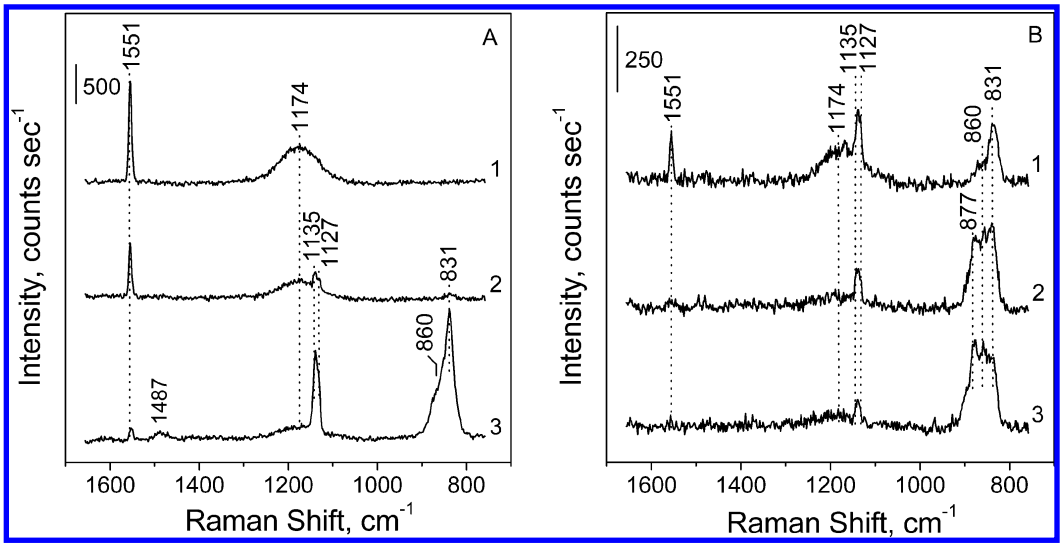

Figure 3. Dioxygen adsorption at 93 K on the CeO_2 pellet reduced with H_2 (A) and CO (B) at 473 (1), 573 (2), or 673 K (3).

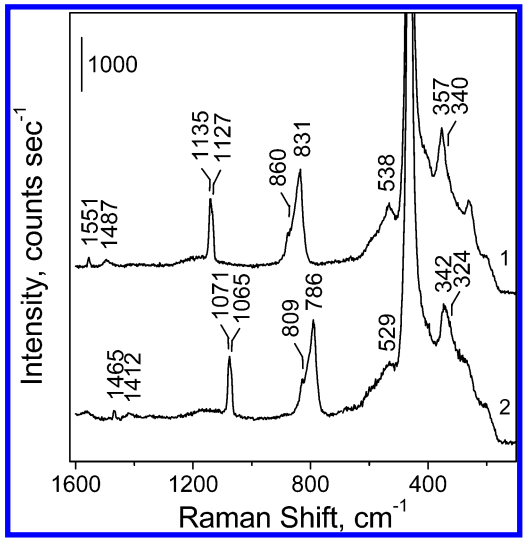

Figure 4. Raman spectra of a CeO_2 pellet reduced with H_2 at 673 K for 1 h before (1) and after adsorption of $^{16}O_2$ (2) or $^{18}O_2$ (3) at 93 K.

K. The CeO_2 band at 1174 cm^{-1} increased during the temperature-programmed oxidation to a maximum value at approximately 550 K. In fact, the thermal stability of the bands associated with adsorption of dioxygen on the CO-reduced CeO_2 was similar in both temperature-programmed experiments. The only major difference was that the stabilities of the bands at 1127 and 1135 cm^{-1} were higher when 10% O_2 in He was used instead of pure He.

The difference in the reactivity of the adsorbed dioxygen species toward CO oxidation is depicted in Figure 7. Exposure of the CeO_2 pellet reduced with H_2 at 623 K to a flow of 10% CO in He at 213 K resulted in the gradual disappearance with time of the band at 1127 cm^{-1}, while the group of the bands centered at 831 cm^{-1} remained intact. There was a measurable reactivity with respect to the bands centered at 831 cm^{-1} only at temperatures above 333 K; the bands at 877 and 860 cm^{-1} were the most reactive (not shown). The interaction of CO with species characterized by vibrational bands at 1127 and 831 cm^{-1} resulted in the formation of surface formate and carbonate species, identified by their FTIR spectra (not shown).

Discussion

Our understanding of electronic defects on the surface of nonstoichiometric CeO_2 has evolved through the use of dioxygen as a probe molecule. Several paramagnetic dioxygen species of different symmetry were characterized by ESR spectroscopy of adsorbed O_2.[8,32−37] The axially symmetric species with both oxygen nuclei equidistant from the surface were assigned to the side-on O_2^- surface complexes[34] and also to the O_2^- species adsorbed on the isolated one-electron surface defects.[35] The species with nonequivalent oxygen atoms were attributed either to the end-on O_2^- species[34] or to the superoxides adsorbed on aggregated vacancies on the CeO_2 surface.[35] However, ESR spectroscopy does not detect diamagnetic peroxides, O_2^{2-}, a common adsorption complex of dioxygen with two-electron defects of oxides surfaces.[5]

Assignments for both superoxide and peroxide species adsorbed on CeO_2 surfaces based on vibrational spectroscopic investigations have been put forth.[35−39] With FTIR and $^{16}O/^{18}O$ isotopic substitution, two bands were previously identified: a band in the range of 1128−1125 cm^{-1} was assigned to an adsorbed superoxide species[35−39] and a band at 883 cm^{-1} was attributed to surface peroxides.[39] For our experiments, the Raman bands in the range of 1200−800 cm^{-1} are present at 1135, 1128, and 831 cm^{-1} and a shoulder at 860 cm^{-1} (Figure 4). The bands at 1135 and 1127 cm^{-1} shifted to 1071 and 1065 cm^{-1}, respectively, when $^{18}O_2$ was adsorbed on the reduced CeO_2 pellet. The observed isotopic shift of 62−64 cm^{-1} is characteristic of O_2^- species[35−39] with an isotopic ratio, $^{16}O_2/^{18}O_2$, of 1.060 and 1.058, respectively.[40] Similarly, the band at 831 cm^{-1} and the shoulder at 860 cm^{-1} shifted to 786 and 809 cm^{-1} (isotopic ratios of 1.057 and 1.063, respectively);[40] the differences in frequencies of 45 and 51 cm^{-1}, respectively, are characteristic of adsorbed peroxide species.[39,41]

It is worth noting that although several different superoxide species on the CeO_2 surface have been identified with ESR spectroscopy,[8,34−37] only one band for the adsorbed O_2^- (ref 42) was detected by FTIR.[35−39] In addition, only one research group has identified spectroscopically peroxide species that form from O_2 adsorption on reduced CeO_2.[39,43] The fact that there are two bands for the superoxides and at least three bands for the peroxides species in the Raman spectra of adsorbed O_2 (Figure 3) may be attributed to the different selection rules of the IR and Raman spectroscopies;[20] highly symmetric complexes of adsorbed dioxygen are typically IR inactive. Thus, the Raman band at 1127 cm^{-1}, an analogue to the band in the range of 1125−1128 cm^{-1} in the IR spectra,[35−39,44] is assigned to the η^1 superoxo species, whereas the band at 1135 cm^{-1} may belong

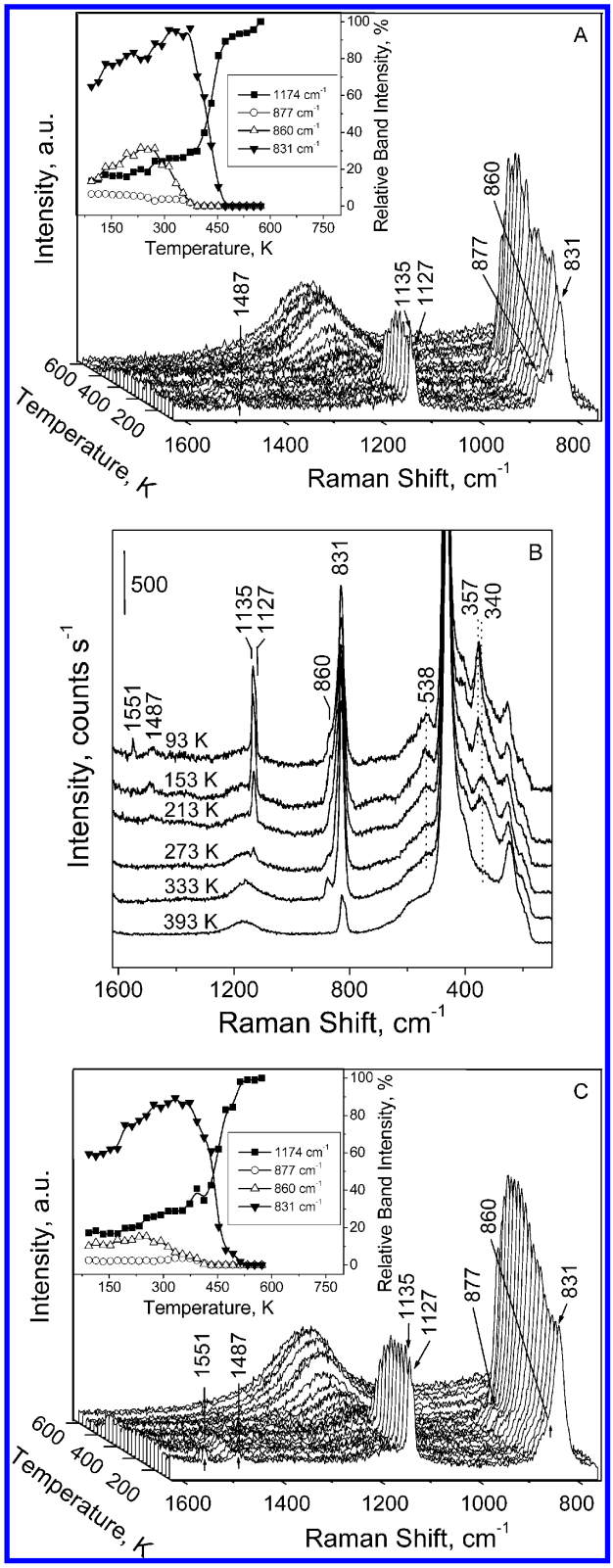

Figure 5. Raman spectra of O_2 adsorbed on a CeO_2 pellet reduced with H_2 at 673 K for 1 h. The spectra were collected in a He (A) and 10% O_2 + He (B) flow at 20 K increments. Dynamics of the normalized band intensity change with temperature are shown in the inset.

to the planar bridging superoxo complexes of O_2 with surface one-electron defects of CeO_2 (Figure 8). The planar bridging superoxo complex may form from the adsorption of an O_2 molecule on the Ce^{3+} ion located next to a coordinatively unsaturated Ce^{4+} ion (possibly a Frenkel-type defect).[45] The bands in the peroxide range of 831−877 cm^{-1} may be attributed to the η^2 peroxo and nonplanar bridging peroxo complexes of adsorbed O_2 with two-electron defects in different local environment (Figure 8).

There is a different ratio between the band intensities of peroxides and superoxides that corresponds to the different relative concentrations of the one- and two-electron defects on the CeO_2 surface reduced with H_2 or CO (Figure 3). This suggests that the mechanism of reduction by CO and H_2 is not the same. Even though two-electron defects on the reduced ceria surface dominate for both reductants, the relative concentration of one-electron defects is much higher for the H_2-reduced CeO_2 (Figure 3). In general, the interaction of an oxide with a CO molecule results in the formation of a CO_2 molecule and an oxygen vacancy on the oxide surface.[46] In the case of CeO_2, reduction with CO leads to the formation of an oxygen vacancy adjacent to the two Ce^{3+} ions, in other words, a two-electron surface defect

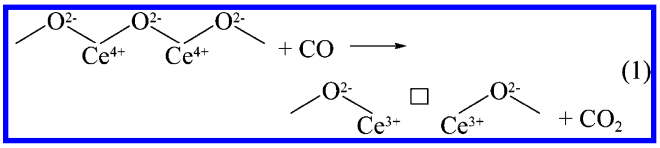

A one-electron defect may form under conditions of CeO_2 reduction with CO via water−gas shift reaction with surface hydroxyl groups[47−50]

$$Ce^{4+}\text{—}OH + CO \longrightarrow Ce^{3+}\square + CO_2 + H \qquad (2)$$

The hydrogen atom evolved in reaction 2 may form a dihydrogen molecule by recombination with another H atom or it may reduce a Ce^{4+} ion to form another one-electron vacancy adjacent to the hydroxyl group

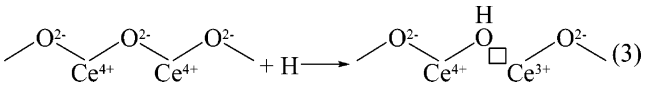

With H_2 reduction, if both H atoms react with the same O atom to form a H_2O molecule, a two-electron vacancy forms, as when CO is the reductant (eq 1). However, the ratio of one-electron defects to two-electron defects is much higher when the CeO_2 is reduced with H_2. This can be understood in terms of the relatively high mobility of H atoms on the CeO_2 surface.[51,52] The rapid diffusion of H atoms apart from each other after the H−H bond dissociates results in the reduction of remote Ce^{4+} ions according to the eq 3.

During the temperature-programmed experiments, reoxidation of the surface by adsorbed oxygen species occurs, independent of the type of carrier gas. Reoxidation is tantamount to the annihilation of the surface defects created by the CeO_2 reduction. The surface reoxidation can be visualized as

$$O_2^-{}_{ads} \rightarrow O_2^{2-}{}_{ads} \rightarrow 2O^-{}_{ads} \rightarrow 2O_2^{2-}{}_{lattice} \qquad (4)$$

The surface superoxides are thermally unstable and convert into peroxides as the temperature increases (Figures 5 and 6). In turn, the peroxides convert into the lattice oxygen resulting in an increase in the intensity of the CeO_2 band at 1174 cm^{-1}. The comparison of the temperature-programmed experiments performed under He and O_2 atmospheres allows one to conclude that gaseous O_2 stabilizes surface superoxide and peroxide species, because the complete reoxidation of CeO_2 occurs at higher temperature under O_2 flow than under He (insets of Figures 5 and 6). To visualize how gas-phase O_2 can inhibit the reoxidation of CeO_2, the participation of bulk oxygen

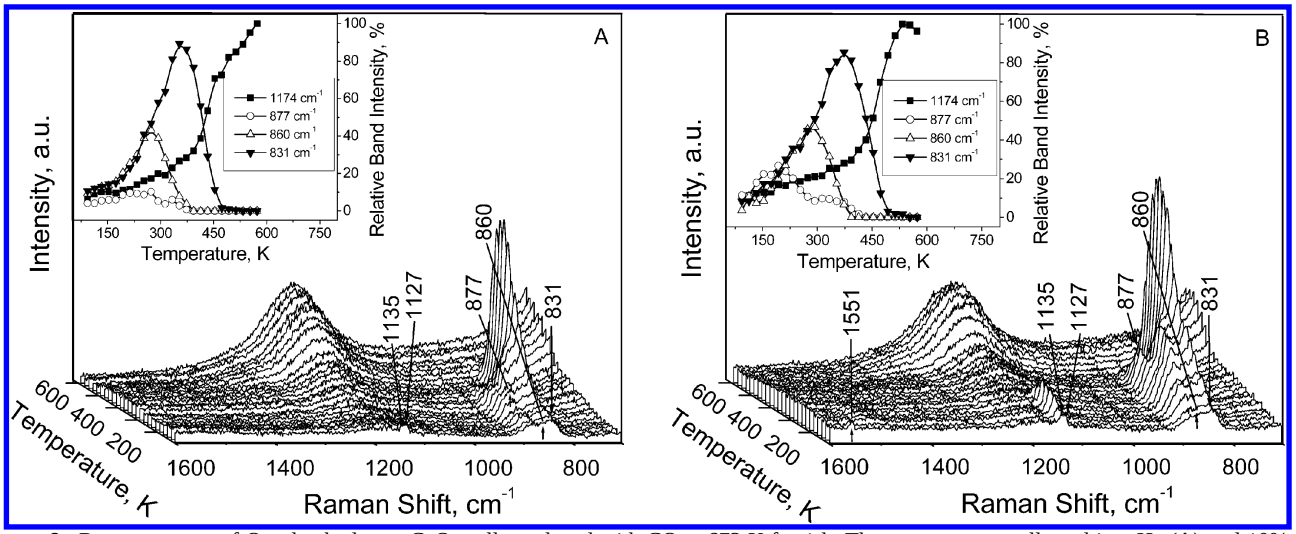

Figure 6. Raman spectra of O_2 adsorbed on a CeO_2 pellet reduced with CO at 673 K for 1 h. The spectra were collected in a He (A) and 10% O_2 + He (B) flow at 20 K increments. Dynamics of the normalized band intensity change with temperature are shown in the inset.

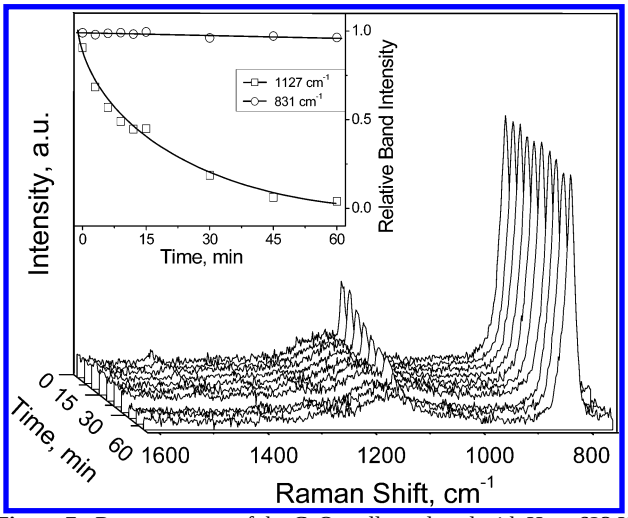

Figure 7. Raman spectra of the CeO_2 pellet reduced with H_2 at 623 K for 1 h followed by O_2 adsorption at 213 K with subsequent exposure to a flow of 10% CO in He at 213 K. Dynamics of the band intensity change with time are shown in the inset.

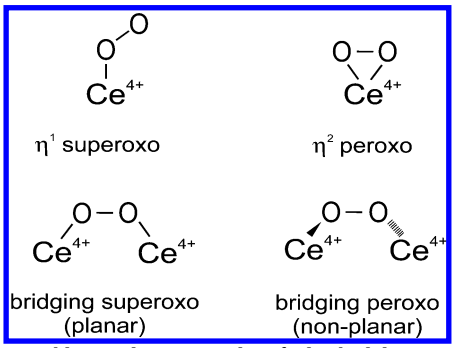

Figure 8. Possible coordination modes of adsorbed dioxygen species.[58]

vacancies must be considered. The supply of oxygen is unlimited during a TPO, and the diffusion of bulk oxygen vacancies to the surface results in the consumption of additional oxygen and a concomitant increase in intensity of the band at 1174 cm^{-1}. The reoxidation is thus determined by the diffusion of the oxygen vacancies, which is not a fast process at moderate temperatures.[27,53] Of course, when the supply of oxygen atoms is limited, as in the case of temperature-programmed experiments in a He flow, the reoxidation process stops when all surface dioxygen species are consumed.

Another feature of the temperature-programmed experiments that is more pronounced for the CO-reduced CeO_2 than the H_2-reduced CeO_2 is the thermal stability of the different peroxide species. As the reoxidation proceeds, the species characterized with an O−O vibrational frequency of 877 cm^{-1} converts into the species with the frequency of 860 cm^{-1}, which then converts into a species with the O−O frequency of 831 cm^{-1} (insets of Figures 5 and 6). The reduced CeO_2 surface contains a set of surface defects (oxygen vacancies) of different degrees of aggregation.[55,56] Reoxidation of the surface decreases the degree of defect aggregation. Concomitantly, the blue frequency shift attributed to dipole−dipole coupling of oscillating species[54] decreases because the number of adjacent adsorbed diatomic species is less. Thus, the highest-frequency band (877 cm^{-1}) is assigned to peroxide species associated with two-electron defects of the most aggregated defect sites. The 860-cm^{-1} band is assigned to peroxide species on two-electron defects that are less aggregated, and the 831-cm^{-1} band is assigned to peroxide species adsorbed on isolated two-electron surface defects. In terms of the model of the defective CeO_2 surface described elsewhere,[55,56] the species characterized by the band at 877 cm^{-1} may be located on triangular defects, whereas peroxides with the band at 860 cm^{-1} may be adsorbed on line defects of the CeO_2 surface.

Further insight into the structure of the adsorbed dioxygen species can be obtained from the analyses of the metal−oxygen bond vibrational region in the Raman spectra (Figures 4 and 5). The bands at 538, 357, and 340 cm^{-1} appear after exposure of a reduced CeO_2 pellet to O_2 and disappear in parallel with the bands of O−O vibration in superoxides and peroxides during TPD (Figure 5B). When $^{18}O_2$ is adsorbed instead of $^{16}O_2$, the bands at 357 and 340 cm^{-1} shifted to 342 and 324 cm^{-1}, respectively (with isotopic ratios of 1.044 and 1.049, respectively). The band at 538 cm^{-1} exhibited an isotopic shift of 9 cm^{-1} (isotopic ratio 1.017); this shift could not be determined precisely because the band was broad and very weak. As surface peroxide species are more thermally stable than superoxides (Figures 5 and 6), we assigned the bands at 538 and 340 cm^{-1} to the asymmetric and symmetric Ce^{4+}−O vibrations of an adsorbed η^2 peroxo complex (Figure 8). The band at 357 cm^{-1} can be attributed to the Ce^{4+}−O vibration of the surface superoxo species. Whether the 357-cm^{-1} band has a higher-frequency counterpart cannot be answered at present, and hence, it is impossible to say if this band is a symmetric vibration in

planar bridging superoxo complexes or it is a $Ce^{4+}-O$ vibration in surface η^1 superoxo complexes (Figure 8). The issue requires further investigation.

The band at 1487 cm^{-1} also deserves consideration. It exhibits an isotopic shift of 75 to 1412 cm^{-1} with $^{18}O_2$ (Figure 4). The isotopic ratio for this band is 1.053. This ratio is lower than that for the O−O vibrational bands of physisorbed dioxygen or adsorbed superoxides and peroxides. The change in the intensity of this band correlates with the change in the intensity of the bands of the superoxide species (Supporting Information, Figures 4 and 5). Thus, we assigned the band at 1487 cm^{-1} to the combination of O−O and $Ce^{4+}-O$ vibrations in surface superoxide complexes.

The nature and the type of dioxygen species adsorbed on the defect sites of oxides surfaces that participate as a principal intermediate still provoke controversy for many oxidation reactions.[57] The results of this investigation show that the superoxide species is more reactive toward CO than the peroxides (Figure 7). Given that the superoxide is a species of radical nature, it is not surprising that the species is more reactive at 213 K. However, at higher temperatures the situation may change. Higher temperatures will favor reaction pathways with higher activation energies, and another oxygen species may become kinetically significant. Thus, the contribution of each of the species shown in the eq 4 into the overall kinetics of CO oxidation catalyzed by CeO_2 at higher temperatures requires further research.

Conclusions

In situ Raman spectroscopy of adsorbed dioxygen was used to characterize electron defects on the surface of nanocrystalline cerium oxide partially reduced with H_2 and CO at different temperatures. By use of $^{16}O/^{18}O$ isotope substitution, the vibrational band at 1551 cm^{-1} after O_2 adsorption at 93 K was attributed to physisorbed O_2 and the bands in the range of 1135−1127 and 877−831 cm^{-1} were assigned to the O−O stretching vibration of the dioxygen species bound to one- and two-electron defects on the CeO_2 surface to form superoxide, O_2^-, and peroxide, O_2^{2-}, species, respectively. The band at 357 cm^{-1} was assigned to the cerium−oxygen vibration of the adsorbed O_2^-, whereas the bands at 538 and 340 cm^{-1} were attributed to the asymmetric and symmetric cerium−oxygen vibration of the adsorbed η^2 peroxo species. On the basis of the comparison of the results of FTIR and Raman spectroscopic investigations, the two bands of superoxide species at 1135 and 1127 cm^{-1} were assigned to the O−O vibration in the planar bridging superoxo and η^1 superoxo dioxygen species. The dynamics of the defect annihilation resulting from the reoxidation of the surface with adsorbed dioxygen species, as measured by temperature-programmed experiments, allowed assignment of the band at 831 cm^{-1} to peroxide species adsorbed on isolated two-electron defects. It was also suggested that the peroxide species characterized by the band at 877 cm^{-1} is located on triangular defects, whereas the peroxide species with the band at 860 cm^{-1} is adsorbed on linear defects of the CeO_2 surface. A mechanism of surface defect formation resulting in different ratios of the one- and two-electron defects on the surface of H_2 and CO reduced CeO_2 was considered. Superoxide species were shown to exhibit much higher reactivity toward CO than peroxides at low temperatures.

Acknowledgment. Support from National Science Foundation (CTS 0086638) and Coordinating Research Council (Grant No E-7a-3) is gratefully acknowledged.

Supporting Information Available: Experimental details referred to in the Experimental Section and figures showing data referred to by numbers in the preceding text are available. This material is available free of charge via the Internet at http://pubs.acs.org.

References and Notes

(1) Liu, G.; Rodriguez, J. A.; Hrbek, J.; Dvorak, J.; Peden, C. H. F. *J. Phys. Chem. B* **2000**, *105*, 7762.
(2) Gellings, P. J.; Bouwmeester, H. J. M. *Catal. Today* **2000**, *58*, 1.
(3) Haber, J. *Stud. Surf. Sci. Catal.* **1997**, *110*, 1.
(4) Trovarelly, A. *Catal. Rev. Sci. Eng.* **1996**, *38*, 439.
(5) Davydov, A. A. *Infrared Spectroscopy of Adsorbed Species on the Surface of Transition Metal Oxides*; John Wiley & Sons: Chichester, 1990.
(6) Dubois, J.-L.; Cameron, C. J. *Appl. Catal. A* **1990**, *67*, 49.
(7) Bensalem, A.; Muller, J.-C.; Tessier, D.; Bozon-Verduraz, F. *J. Chem. Soc., Faraday Trans.* **1996**, *92*, 3233.
(8) Martínez-Arias, A.; Soria, J.; Conesa, J. C.; Seoane X. L.; Arcoya, A.; Cataluña, R. *J. Chem. Soc., Faraday Trans.* **1995**, *91*, 1679.
(9) Fornasiero, P.; Kaspar, J. *Collect. Czech. Chem. Commun.* **2001**, *66*, 1287.
(10) Niwa, M.; Furukawa, Y.; Murakami, Y. *J. Colloid Interface Sci.* **1982**, *86*, 260.
(11) Nakamoto, K. *Infrared and Raman Spectra of Inorganic and Coordination Compounds: Part B*, 5th ed.; John Wiley & Sons: New York, 1997.
(12) Binet, C.; Daturi, M.; Lavalley, J.-C. *Catal. Today* **1999**, *50*, 207.
(13) Haber, J.; Turek, W. *J. Catal.* **2000**, *190*, 320.
(14) Lunsford, J. H. *Angew. Chem., Int. Ed. Engl.* **1995**, *34*, 970.
(15) Wang, J. A.; Valenzuela, M. A.; Castillo, S.; Salmones, J.; Moran-Pineda, M. *J. Sol−Gel Sci. Technol.* **2003**, *26*, 879.
(16) Pengpanich, S.; Meeyoo, V.; Rirksomboon, T.; Bunyakiat, K. *Appl. Catal. A* **2002**, *234*, 221.
(17) Wong, G. S.; Concepcion, M. R.; Vohs, J. M. *J. Phys. Chem. B* **2002**, *106*, 6451.
(18) Roh, H.-S.; Jun, K.-W.; Baek, S.-C.; Park, S.-E. *Chem. Lett.* **2001**, 1048.
(19) Kaspar, J.; Fornaciero, P.; Graziani, M. *Catal. Today* **1999**, *50*, 285.
(20) Nakamoto, K. *Infrared and Raman Spectra of Inorganic and Coordination Compounds: Part A*, 5th ed.; John Wiley & Sons: New York, 1997.
(21) Gu, X. J. *J. Raman Spectrosc.* **1996**, *27*, 83.
(22) Weber, W. H.; Hass, K. C.; McBride, J. R. *Phys. Rev. B.* **1993**, *48*, 178.
(23) Twu, J.; Chuang, C. J.; Chang, K. I.; Yang, C. H.; Chen, K. H. *Appl. Catal., B.* **1997**, *12*, 309.
(24) Yao, H. C.; Yu Yao, Y. F. *J. Catal.* **1984**, *86*, 254.
(25) Badri, A.; Binet, C.; Saussey, J.; Lavalley, J.-C. *Mikrochim. Acta* **1997**, *14*, 697.
(26) Binet, C.; Badri, A.; Lavalley, J.-C. *J. Phys. Chem.* **1994**, *98*, 6392.
(27) Daturi, M.; Finoccho, E.; Binet, C.; Lavalley, J. C.; Fally, F.; Perrichon, V. *J. Phys. Chem. B* **1999**, *103*, 4884.
(28) Perrichon, V.; Laachir, A.; Bergeret, G.; Fréty, R.; Tournayan, L.; Touret, O. *J. Chem. Soc., Faraday Trans.* **1994**, *90*, 773.
(29) Badri, A.; Binet, C.; Lavalley, J.-C. *J. Chem. Soc., Faraday Trans.* **1996**, *92*, 4669.
(30) The low-intensity bands at 2254, 1702, and 1654 cm^{-1} were also observed. They were assigned to the first overtones of the bands at 1135−1127 and 877−831 cm^{-1}, respectively.
(31) Zhanpeisov, N. U.; Staemmler, V.; Baerns, M. *J. Mol. Catal.* **1995**, *101*, 51.
(32) Che, M.; Kibblewhite, J. F. J.; Tench, A. J.; Harwell, A. E. R. E.; Dufaux, M.; Nacchache, C. *J. Chem. Soc., Faraday Trans. 1* **1973**, *69*, 857.
(33) Rojo, J. M.; Sanz, J.; Soria, J. A.; Fierro, J. L. G. *Z. Phys. Chem. N. F.* **1987**, *152*, 149.
(34) Zhang, X.; Klabunde, K. J. *Inorg. Chem.* **1992**, *31*, 1706.
(35) Soria, J.; Martínez-Arias, A.; Conesa, J. C. *J. Chem. Soc., Faraday Trans.* **1995**, *91*, 1669.
(36) Haneda, M.; Mizushima, T.; Kakuta, N. *J. Chem. Soc., Faraday Trans.* **1995**, *91*, 4459.
(37) Soria, J.; Coronado, J. M.; Conesa, J. C. *J. Chem. Soc., Faraday Trans.* **1996**, *92*, 1619.
(38) Li, C.; Domen, K.; Maruya, K.-I.; Onishi, T. *J. Chem. Soc., Chem. Commun.* **1988**, 1541.
(39) Li, C.; Domen, K.; Maruya, K.-I.; Onishi, T. *J. Am. Chem. Soc.* **1989**, *111*, 7683.
(40) The calculated value is 1.060.
(41) Li, W.; Gibbs, G. V.; Oyama, S. T. *J. Am. Chem. Soc.* **1998**, *120*, 9041.

(42) Another weak band at 1145 cm^{-1} in addition to that at 1126 cm^{-1} was detected in the FTIR spectra of an alumina-supported CeO_2 (ref 37). However, attempts to assign this band with $^{18}O_2$ adsorption were unsuccessful because of very low band intensity.

(43) Li, C.; Domen, K.; Maruya, K.-I.; Onishi, T. *J. Catal.* **1990**, *123*, 436.

(44) Bulanin, K. M.; Lavalley, J. C.; Lamotte, J.; Mariey, L.; Tsyganenko, N. M.; Tsyganenko, A. A. *J. Phys. Chem. B* **1998**, *102*, 6809.

(45) Mamontov, E.; Dmowski, W.; Egami, T.; Kao, C.-C. *J. Phys. Chem. Solids*. **2000**, *61*, 431.

(46) Boreskov, G. K. *Catal. Sci. Technol.* **1982**, *3*, 39.

(47) Barbier Jr., J.; Duprez, D. *Appl. Catal., B.* **1993**, *3*, 61.

(48) Taha, R.; Martin, D.; Kacimi, S.; Duprez, D. *Catal. Today* **1996**, *29*, 89.

(49) Holmgren, A.; Andersson, B. *J. Catal.* **1998**, *178*, 14.

(50) Holmgren, A.; Andersson, B.; Duprez, D. *Appl. Catal. B.* **1999**, *22*, 215.

(51) Duprez, D. *Stud. Surf. Sci. Catal.* **1997**, *112*, 13.

(52) Martin, D.; Duprez, D. *J. Phys. Chem. B* **1997**, *101*, 4428.

(53) Martin, D.; Duprez, D. *J. Phys. Chem.* **1996**, *100*, 9429.

(54) Ueba, H. *Surf. Sci.* **1987**, *188*, 421.

(55) Fukui, K.-I.; Namai, Y.; Iwasawa, Y. *Appl. Surf. Sci.* **2002**, *188*, 252.

(56) Nörenberg, H.; Briggs, G. A. D. *Surf. Sci.* **1999**, *424*, L352.

(57) See, for example: Zhang, H. B.; Lin, G. D.; Wan, H. L.; Liu, Y. D.; Weng, W. Z.; Cai, J. X.; Shen, Y. F.; Tsai, K. R. *Catal. Lett.* **2001**, *73*, 141 and references therein.

(58) It is worth emphasizing that the main difference between bridging superoxo and peroxo complexes is that the former complex forms resulting from O_2 adsorption on a Ce^{3+} ion adjacent to a coordinatively unsaturated Ce^{4+} ion, whereas the latter complex forms via adsorption of a O_2 molecule on two adjacent Ce^{3+} ions. Hence, even though the structures of the bridged superoxo and peroxo complexes may look similar, the eletronic configuration of the oxygen atoms is different, resulting in different IR spectra.